*Journal of the Korean Nuclear Society*
*Volume 21, Number 1, March, 1989*

# Particle Simulation Modelling of a Beam Forming Structure in Negative-Ion-Based Neutral Beam Injector

**Byoung-Lyong Choi and Sang Hee Hong**

Seoul National University

(Received August 22, 1988)

# 중성빔 입사장치에서 빔형성 구조의 입자모사 모형

**최병룡 · 홍상희**

서울대학교

(1988. 8. 22. 접수)

## Abstract

For the effective design of a beam forming structure of the negative-ion-based neutral beam injector, a comquter program based on a particle simulation model is developed for the calculation of charged particle motions in the electrostatic fields. The motions of negative ions inside the acceleration tube of a multiple-aperture triode are computed at finite time steps. The electrostatic potentials are obtained from the Poisson's equation by the finite difference method. The successive overrelaxation method is used to solve the matrix equation. The particle and force weighting methods are used on a cloud-in-cell model. The optimum design of the beam forming structure has been studied by using this computer code for the various conditions of elctrodes. The effects of the acceleration-deceleration gap distance, the thickness of the deceleration electrode and the shape of the acceleration electrode on beam trajectories are exmined to find the minimum beam divergence. Some numerical illustrations are presented for the particle movements at finite time steps in the beam forming tubes. It is found in this particle simulation modelling that the shape of the acceleration electrode is the most sign ificant factor of beam divergence.

## 요 약

중성 입자 입사 장치의 효율적인 빔형성 구조를 목적으로 정전기장 내에서 하전 입자의 움직임을 시간의 흐름에 따라 계산해 볼 수 있는 프로그램을 만들어 입자 모사 모형을 찾았다.

가속관 내의 입자의 움직임은 일정 시간 간격으로 계산하였고 전위는 유한차분법에 의해 Poisson 방정식에서 구하였다. 행렬식은 반복해법인 successive overrelaxation법을 사용하였고 전하밀도와 입자에 미치는 전기장의 힘을 구할 때는 cloud-in-cell 모델을 사용하였다. 이 전자계산 코드를 사용하여 가속관 내 전극의 여러 조건들을 변화시켜가면서 빔형성 구조의 최적설계를 수행하였다. 중성자 입사 장치의 가속관에서 가속 감속-전극간의 간격 변화, 감속전극의 두께 변화, 가속 전극의 형태 변화 등을 통하여 이들이 빔의 모양에 끼치는 영향을 조사하여 몇가지 경우에 있어서 일정한 시간 간격으로 나타나는 입자들의 움직임을 예시하였다. 이 입자 모사모형을 통하여 가속전극의 형태가 빔 퍼짐에 가장 주요한 역할을 하는 것을 알았다.

## 1. Introduction

At the primary-heating stage of tokamak operation the plama temperature can be raised by an Ohmic heating method. However, as the temperature rises, the resistivity $\eta$ decreases as $T^{-3/2}$, so that Ohmic heating becomes less and less efficient to heat the plasma. At the same time, the power losses due to bremsstrahlung increase as $T^{1/2}$, and consequently the radiative losses overcome Ohmic heating at some point of heating period. Since the plasma current density j is limited by the MHD instability, the power density $\eta j^2$ from Ohmic heating also has a limit. Hence this heating approach quickly reaches a point of diminishing returns, and other means of heating the plasma to reactor conditions have to be found.[1-3] The various auxiliary heating methods have been proposed, and to date the most feasible methods are radiofrequency (RE) heating, adiabatic compression heating, and neutral beam injection heating.[1-6] For the neutral beam heating of the tokamak, a high current ion beam, typically in 20~100 keV and 200~2000 kW ranges, is accelerated by a multiaperture ion source and is converted to a neutral atom beam by the charge exchange in a gas cell.

Fig.1 shows a schematic diagram of a neutral beam injector for the SNUT-79 tokamak in our laboratory.[7] Particularly the beam forming element of the system, i.e., the accelerator, makes the H ion beam accelerate up to the desired particle energy and travel in parallel with the accelerator tube axis. In the design it is required to minimize the divergence of the accelerated beam and to handle large total ion currents in the range of several hundred amperes.

In this work the motions of ions inside the accelerator of the neutral beam injector are found as time passes by the particle simulation method for electrostatic systems. The electrostatic potentials are obtained from the Poisson's equation by the finite difference method, and the motions of negative ions inside the beam forming tube of a multiple-aperture triode are computed at finite time steps. The successive overrelaxation method is used to solve the matrix equation, and the

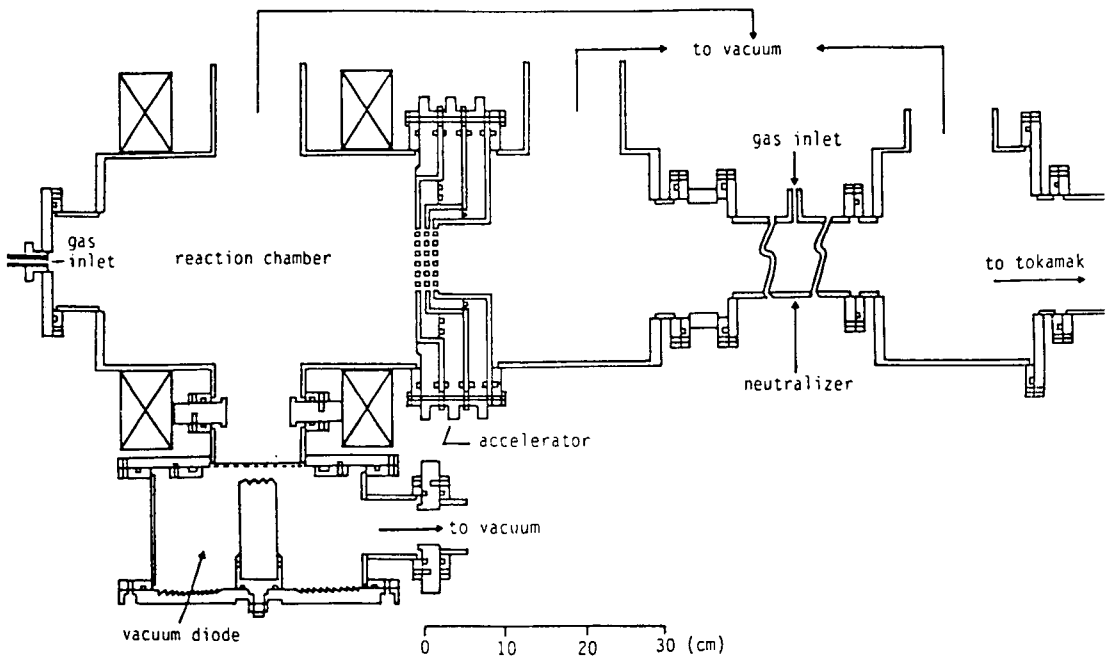


**Fig.1 Neutral Beam Injector for SNUT-79 Tokamak.**

particle and force weighting methods are adopted for a cloud-in-cell model. The effects of the acceleration-deceleration gap distance, the thickness of the deceleration electrode, and the shape of the acceleration electrode on beam trajectories are examined by the calculations obtained from the particle simulation. As a result an optimum design of the beam forming structure for the negative-ion-based neutral beam injector is found to minimize the divergence of the negative hydrogen ion beam.

## 2. Electrostatic Programs

### 2.1. Overview of computational procedure

The charged particles in the beam forming structure of the neutral beam injector move by the forces produced by their own and applied electric fields. The initial conditions for particle positions and velocities are given at the initial time, and the boundary conditions for the electrostatic potentials are prescribed at the electrode boundaries. The fields in the accelerator are calculated from the initial charge densities by the Poisson's equation. The particle movements are then found in these fields by finding the forces exerting on particles from the single-particle equations of motion. Next, the changed electric fields due to charged particles at new positions and velocities are recalculated.

This procedure is repeated for the prescribed time steps. In this process, to obtain the field quantities, it is necessary to do some weighting to the grid points, which is dependent on the particle position. After the fields are calculated at the grid points, the electric fields generating the force on the particles are interpolated from the grid fields by performing a weighting again. Fig.2 shows an overall scheme of the computational procedure.

### 2.2. Integration of equations of motion

Two first-order differential equations integrated separately for each particle are

$$m\frac{d\mathbf{v}}{dt}=\mathbf{F},\ \frac{d\mathbf{x}}{dt}=\mathbf{v}, \tag{1}$$

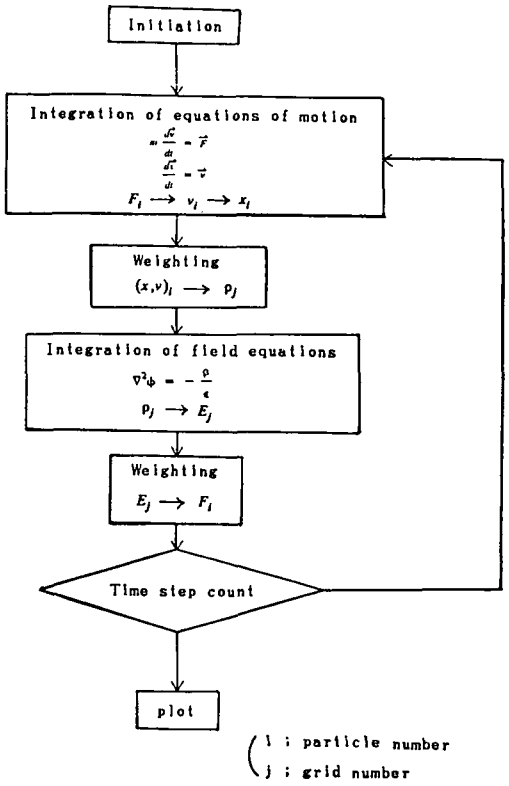


Fig.2 Overall Scheme of Computational Procedure.

These equations are replaced by the finite difference equations:

$$m\frac{\mathbf{v}_{new}-\mathbf{v}_{old}}{\triangle t}=\mathbf{F}_{old}, \tag{2}$$

$$\frac{\mathbf{x}_{new}-\mathbf{x}_{old}}{\triangle t}=\mathbf{v}_{new}.$$

In this replacement the leap-frog method is used because of its simplicity and accuracy.[8] The particle movements in time and the time-centering are depicted for the leap-frog method in Fig.3. The calculations advance from $\mathbf{v}_{t-\Delta t/2}$ and $\mathbf{x}_t$ to $\mathbf{v}_{t+\Delta t/2}$ and $\chi_{t+\Delta t}$ respectively, even though $\mathbf{v}$ and $\mathbf{x}$ are not known at the same time. Initially, $\mathbf{v}(o)$ is pushed back to

$$\mathbf{v}(-\frac{\triangle_t}{2}).$$

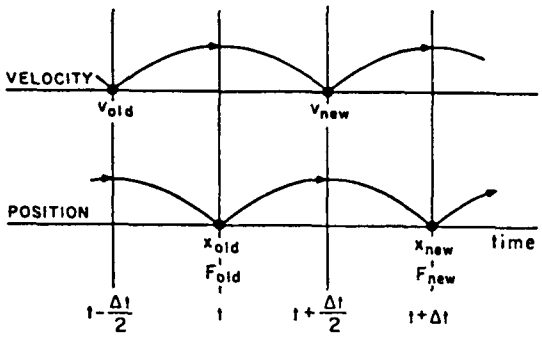


Fig.3 Leap-Frog Method.

### 2.3. Integration of field equations

The electric fields are obtained from Maxwell's equations by assigning charge densities to grid points in the accelerator. The accelerator can be considered as an electrostatic system, in which the electric field **E** is determined by the electrostatic potential $\phi$ so that

$$\mathbf{E}=\nabla\phi, \tag{3}$$

since $\nabla\times\mathbf{E}=-\frac{\partial\mathbf{B}}{\partial t}=0$, Substitution of Eq.(3) into Gauss' law yields the Poisson's equation;

$$\nabla^2\phi=-\frac{\rho}{\varepsilon}, \tag{4}$$

where $\varepsilon$ is the electrical permittivity, and $\rho$ the charge density.

The finite difference form of Eq.(4) can be written in a two-dimensional beam forming structure as

$$\frac{\phi_{r+1,s}-2\phi_{r,s}+\phi_{r-1,s}}{hx^2}+\frac{\phi_{r,s+1}-2\phi_{r,s}+\phi_{r,s-1}}{hx^2}=-\frac{\rho(x_r,y_s)}{\varepsilon}, \tag{5}$$

where r and s designate the grid points, and $h_x$ and $h_y$ are the grid intervals in x and y directions, respectively. This equation is to be solved by the successive overrexation method in the iterative scheme.

### 2.4. Weighting methods for particle and force

It is necessary for the determination of the electric fields at the grids to calculate the charge densities at the grid points by knowing the charged particle positions. calculations of the forces exerting on the particles are carried out after the electric fields at the grids are obtained. These calculations are called weighting, and they imply some form of interpolation among the grid points nearest to the particle. It needs some care to use the same weighting in both the density and force calculations in order to avoid a self-force.

One of the weighting methods is the zero-size-particle and nearest-grid-point method (ZSP-NGP),[9] which is inaccurate due to the noise at the space and the time. The cloud-in-cell (CIC) weighting[10] has thus been picked up in this work. In the CIC method the particle coordinates (x,y) are taken to be at center-of-mass and center-of-charge of charged clouds of finite extent. The particles have finite size, are tenuous, and may pass through one another. Thus, the particles are called clouds. The charge density to be assigned to the points in a spatial grid is obtained by sharing the charges at several points by linear interpolations. For a large mumber of clouds, the charge density at an (i,j) grid point is obtained by summing over the clouds as

$$\rho(i,j)=\sum A_{ij}\rho_c(x,y), \tag{6}$$

where $\rho_c(x,y)$ is the density of the cloud at (x,y), and $A_{ij}$ is the area of the cloud appearing in the cell centered at i,j divided by the area of the cell. The cloud size is taken as that of the cell size in this work. In case of Fig.4, the weights for charge densities are given by

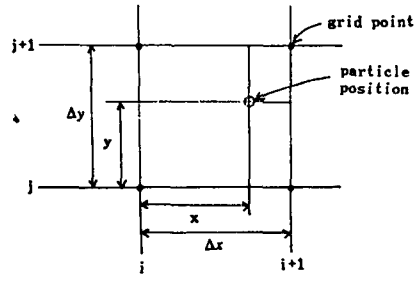


Fig.4 Assignment of Charge Density to Grid Points for CIC Model.

$$\rho(i,j)=\rho_t\frac{(\triangle x-x)(\triangle y-y)}{\triangle x\triangle y}$$

$$\rho(i+1,j)=\rho_t\frac{x(\triangle y-y)}{\triangle x\triangle y}, \quad (7)$$

$$\rho(i+1,j+1)=\rho_t\frac{xy}{\triangle x\triangle y},$$

$$\rho(i,j+1)=\rho_t\frac{(\triangle x-x)y,}{\triangle x\triangle y},$$

where $\rho_t$ is the charge density uniformly filling a cell (Coulomb/cell), and the charge position (x,y) is measured from the lower left-hand grid point.

For the force weighting the CIC method uses the electric force on a cloud as that averaged over the cloud as given by

$$\mathbf{E}(x,y)_{effective}=\sum_{cloud}A_{ij}\mathbf{E}_p \quad (8)$$

The $\mathbf{E}_p$ are the fields at the grid points where the parts of the cloud are assigned.

## 3. Beam Forming Structure Design

### 3.1. Design consideration

In designing the accelerator, a careful attention has to be paid to the fact that the extraction ion beam current I is inversely proportional to the square of the gap distance d between the electrodes, and that the aperture diameter is less than or equal to d to minimize the extraction beam divergence. For this reason the multiple aperture electrode is used for large current, and the items which must be considered in the design of the beam forming structure are[11]

(1) Beam energy and power,
(2) the number and the gap distance of the electrodes,
(3) transparency of the extraction aperture to the extraction plane,
(4) beam divergence.

The beam energy is high enough to assure the adequate penetration into the plasma before ionization and trapping occur, but not so high that a substantial fraction transverses completely and is wasted or causes demage on the other side of the container. The beam power is high enough to provide the desired heating of the plasma. For the number and the gap distance of the electrodes affect the beam divergence, these relevant facts are to be determined. The transparency of the extraction aperture to the extraction plane has effects on the beam current, electrode heating, and electric field shape.

### 3.2. Design parameters

The beam energy depends on the direction of the neutral beam injection and the thickness of plasma. In case of the perpendicular injection, the beam penetration thickness D is $\overline{na}$ where $n(cm^{-3})$ is the plasma density and a(cm) is the plasma radius. In consequence of the experiment[12-14]

$$D=5.5\times10^{10}E_0(cm^{-2}), \quad (9)$$

where $E_0$(eV) is the beam energy,

$$E_0=1.82\times10^{-11}\overline{na}. \quad (10)$$

Therefore the plasma density and the minor radius determine the injection beam energy. The power needed to sustain a plasma volume V( $l$ ) with a mean density $\bar{n}(cm^{-3})$, ion and electron temperatures Ti and Te (keV), and the energy confinement time $\tau$(ms) is given by

$$P(kW)=2.4\times10^{13}\bar{n}(T_i+T_e)V/\tau \quad (11)$$

The beam energies of 15~20keV are used in this particle simulation accelerator design. The plasma density of $10^{13}$ $cm^{-3}$, the plasma temperature of 100eV, the plasma volume of 500 liters, and the energy confinement time of 10 ms are taken in the simulation for the SNUT-79 tokamak. With these values and Eq. (11) the beam power required becomes 24kW.

The transparency of the extraction aperture to the extraction plane is considered to be 40~50%. Generally the diode is used for several keV, the triode is used

for scores of keV, and the tetrode is used for the beam energy more than 100keV. For the SNUT-79 tokamak the beam energy is 3~30keV so that the triode is taken for the number of electrodes. By experiment the relation between discharge voltage $V_b$ and gap distance d for the triode is

$$V_b=(8\times10^4\sim10^5)d. \quad (12)$$

The triode has three electrodes which are the acceleration electrode, the deceleration electrode, and the ground electrode. The acceleration-deceleration gap distance has to be greater than 2.5mm by Eq.(12)

With the design parameters mentioned above, various electrode shapes and the arrangements of electrodes are experimented by the computer simulation to minimize the ion beam divergence.

## 4. Results and Discussions

The effective design of the beam forming tube of the neutral beam injector has been performed by making use of a computer code developed in this work by changing three factors in proper order. At first stage, the alteration of the deceleration electrode positions is made. The effect of the deceleration electrode thickness is considered at second stage. Finally the shapes of the acceleration electrode are varied while the position and thickness of the deceleration electrode are fixed. The parameters used in this calculation are listed in Table 1.

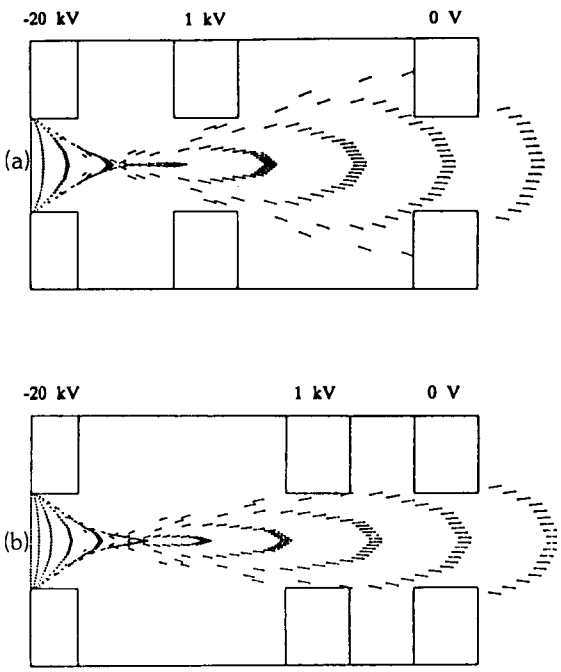


**Fig.5 Effect of Deceleration Electrode Position on Particle Movements at Finite Time Steps.**

Fig.5 shows the motions of the particles as the deceleration electrode positions are varied. The system consists of the acceleration electrode and the ground electrode, -20kV and 0V, respectively, and deceleration electrode of 1kV. Each beam-path column appeared from the left side shows the motions of the particles at each finite time step. The heads and lengths of the arrows indicate the directions and normalized magni-

**Table 1 Parameters Used for Calculations**

| | |
|---|---|
| Number of hydrogen negative-ion particles | 32 |
| Physical length of system | $1.4\times10^{-2}$m, $8\times10^{-3}$m |
| Number of grids | 28×16 or 56×32 |
| Proceeding time | $10^{-9}$s |
| Number of time steps to run | 30 |
| Initial velocity of particles of 10eV | $3.093\times10^4$ m/s |
| Plotting interval | $2\times10^{-9}$s |

tudes of the negative ion velocities, respectively. The number of grids used in the calculation is 28×16. In Fig.5(a), the deceleration electrode is close to the acceleration electrode as possible as it can. It can be easily seen that the diverge of the particles as time passes is severe. In Fig.5(b) where the deceleration electrode is moved toward the ground electrode, the tendency of divergence is improved. In consequence of calculating the various cases, it is found that the position of the deceleration electrode is appropriate at 2/3 of the gap between acceleration and ground electrodes.

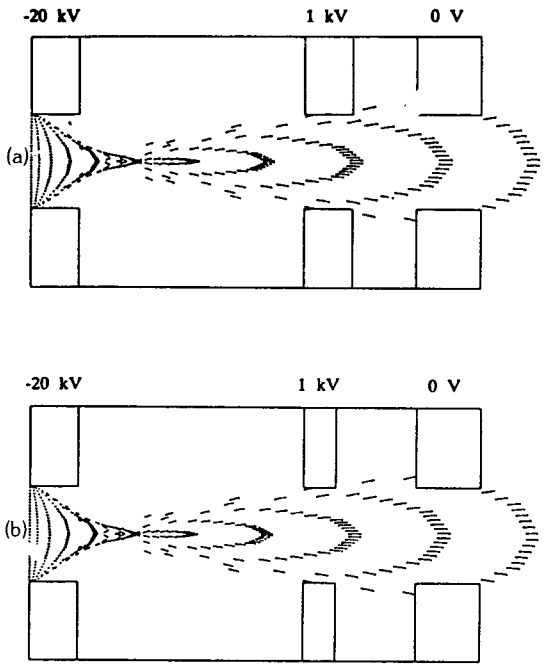


Fig.6 Effect of Deceleration Electrode Thickness on Particle Movements at Finite Time Steps.

Fig.6 tells the effect of the deceleration electrode thickness while the deceleration electrodes are placed on the same positions. It is seen in this figure that the positions and the velocities of the particles are not changed with the deceleration electrode thicknesses. The results show that the thickness of the deceleration electrode does not affect the motions of the particles.

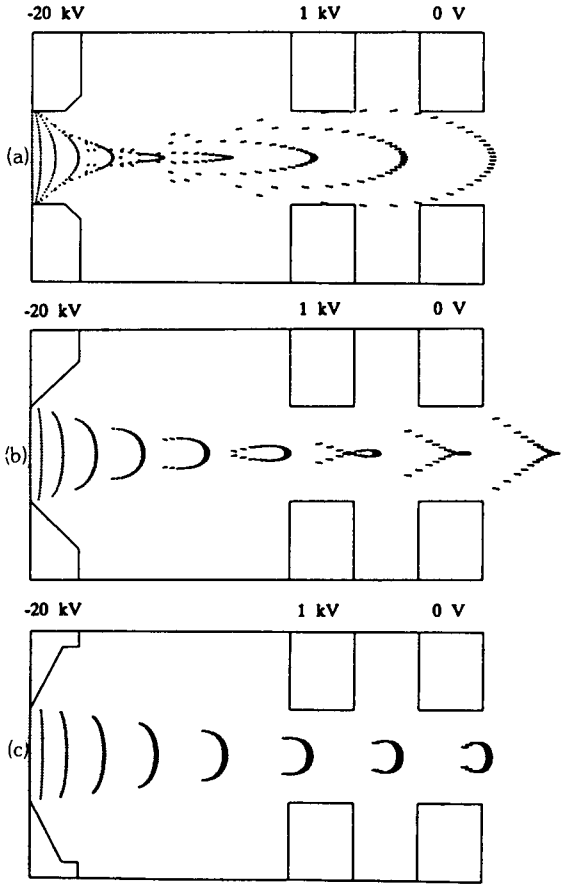


Fig.7 Effect of Acceleration Electrode Shape on Particle Movements at Finite Time Steps.

The effect of the acceleration electrode shape is considered in Fig.7, in which the number of grids used in the calculations is 56×32 to make the accelerator electrode shape diverse. The corner of the acceleration electrode is cut a little in Fig.7(a), and the results show that the divergence diminshes. In Fig.7(b), the corner of the acceleration electrode is cut wholly. The waist of the beam is formed near the deceleration electrode, and the beam divergence is improved markedly. But there are some diverging particles at the beam edge and they will leave the designed path during the motion toward the port of the tokamak, When one desires to determine the shape of the acceleration electrode, the fabrication has the be considered. The hole of the acceleration electrode is made by a drill,

and one of the shape that can be made is shown in Fig.7(c). In this case the waist of the beam is not seen in the acceleration tube and the beam form is much improved. Also the equipotential lines are flatter and smoother than before. Consequently it is concluded that the shape of the acceleration electrode has the most significant effect on the beam form and divergence, and that the beam forming structure of the injector in Fig.7(c) is desirable for the effective neutral beam injection.

## 5. Conclusions

A computer program calculating the motions of charged particles in the electrostatic field is made, and a particle simulation model is found for the optimum design of the beam forming structure of the neutral beam injection system used for the the auxiliary heating fo a tokamak.

It is found in this particle simulation modelling that i ) the position of deceleration electrode is appropriate at 2/3 of the acceleration-ground electrode gap for minimizing the divergence fo the particles, ii ) the effect of the thickness of the deceleration electrode can be negligible to the motions of the particles, and iii) the shape of the acceleration electrode has the most significant effect on the beam forming and divergence. A hat-shaped acceleration electrode shown in Fig.7(c) is desirable for the effective neutral beam injection.

## References

1. W.M.Stacey, Jr., Fusion Plasma Analysis, John Wiley, New York, 1981
2. A.Gibson et al., Nucl. Fusion 27, 481 (1987)
3. T.J.dolan, Fusion Research, Pergamon, New York, 1982.
4. H.Koepfel and G.Mazzitelli, Heating in Toroidal Plasmas, Rep. on the 4th Intl. Sympo., Rome, 1984.
5. H.H.Haselton and R.V.Pyle, in Proc. 4th Topical meeting on tech. of control. Nucl. Fusion, 81, King of Prussia, USA, 1980.
6. E. Teller, Magnetic Confinement, Academic, New York, 1981.
7. S.M.Hwang, Ph.D.Thesis, Seoul National University, 1987.
8. C.K.Birdsall and A.B.Landon, Plasma Physics via Computer Simulation, McGraw-Hill, New York, 1985.
9. R.W.Hockey, Phys. Fluids 9, 1862.(1966).
10. C.K.Birdsall and D.Fuss, J.Comput. Phys. 3, 49 4(1969).
11. D.A.Brouchous and J.R.Conrad, Rev.Sci. Instrum. 53, 1181. (1982).
12. J.D.Callen and J.A.Rome, Nucl. Fusion 20, 501 (1980)
13. D.R. Sweetman, Nucl. Fusion 13, 157(1973).
14. M.M.Menon, Proc. IEEE 69. 1012 (1981).